

Evaporating Heat Transfer Characteristics of R-134a in a Horizontal Smooth Channel

A. S. Pamitran, Kwang-Il Choi, Jong-Taek Oh[†], Hoo-Kyu Oh^{**}

Graduate School, Department of Refrigeration Engineering, Chonnam National University, Yeosu 550-749, Korea

^{*}*Department of Refrigeration Engineering, Chonnam National University, Yeosu 550-749, Korea*

^{**}*Department of Refrigeration and A/C Engineering, Pukyong National University, Busan 608-739, Korea*

Key words: R-134a, Flow boiling, Flow pattern, Heat transfer coefficient, Horizontal minichannel

ABSTRACT: Convective boiling heat transfer coefficients were measured in a horizontal mini-channel with R-134a. The test section was made of stainless steel tube with an inner diameter of 3.0 mm and a length of 2 m. It was uniformly heated by applying electric current directly to the tube. Local heat transfer coefficients were obtained for heat fluxes from 10 to 40 kW/m², mass fluxes from 200 to 600 kg/m²s, qualities up to 1.0, and the inlet saturation temperature of 10°C. The experimental results were mapped on Wojtan et al.'s⁽⁷⁾ and Wang et al.'s⁽⁸⁾ flow pattern maps. The nucleate boiling was predominant at low vapor quality whereas the convective boiling was predominant at high vapor quality. Laminar flow appeared in the flow with minichannel. The experimental results were compared with six existing two-phase heat transfer coefficient correlations. A new boiling heat transfer coefficient correlation based on the superposition model for refrigerants was developed with mean and average deviations of 10.39% and -3.66%, respectively.

Nomenclature

<p>A : average deviation,</p> $A = \frac{1}{n} \sum_1^n \frac{(h_{pred} - h_{exp}) \times 100}{h_{exp}}$ <p>Bo : Boiling number</p> <p>C : Chisholm parameter</p> <p>C_p : specific heat [kJ/kgK]</p> <p>D : diameter [m]</p> <p>dp/dz : pressure gradient [N/m²m]</p> <p>F : convective two-phase multiplier</p> <p>f : friction factor</p> <p>fn : function</p> <p>G : mass flux [kg/m²s]</p> <p>h : heat transfer coefficient [kW/m²K]</p> <p>i : enthalpy [kJ/kg]</p>	<p>k : thermal conductivity [kW/mK]</p> <p>L : length of test section [m]</p> <p>M : mean deviation,</p> $M = \frac{1}{n} \sum_1^n \left \frac{(h_{pred} - h_{exp}) \times 100}{h_{exp}} \right $ <p>M : molecular weight (Eq. 11) [kg/kmol]</p> <p>P : pressure [kPa]</p> <p>Q : electric power [kW]</p> <p>q : heat flux [kW/m²]</p> <p>S : suppression factor of nucleate boiling</p> <p>T : temperature [K]</p> <p>W : mass flow rate [kg/s]</p> <p>X : Martinelli parameter</p> <p>x : mass quality</p> <p>z : axial coordinate [m]</p>
--	---

† Corresponding author

Tel.: +82-61-659-3273; fax: +82-61-659-3003

E-mail address: ohjt@chonnam.ac.kr

Greek symbols

μ : dynamic viscosity [Ns/m²]

- ρ : density [kg/m^3]
 ϕ^2 : two-phase frictional multiplier

Subscripts

- crit* : critical point
exp : experimental value
f : saturated liquid
g : saturated vapor
i : physical property based on inlet temperature (Eqs. 4 and 5)
i : inner tube
lo : liquid only
nbc : nucleate boiling contribution
o : outer tube
pb : pool boiling
pred : prediction value
r : reduced
sat : saturation
sc : subcooled
t : turbulent
tp : two-phase
v : laminar
w : wall

1. Introduction

Two-phase flow heat transfer has been a research subject for several decades, but only a few study in the literature was reported on two-phase heat transfer of refrigerants in minichannel. Published data relating to two-phase flow and heat transfer in small channels are relatively few, compared to data for large channels.

This study was undertaken to obtain experimental data for refrigerant R-134a and determine the local heat transfer coefficient during evaporation in a minichannel. The experimental results were compared against six existing two-phase boiling heat transfer coefficient prediction methods, by Wattelet et al.,⁽¹⁾ Shah,⁽²⁾ Tran et al.,⁽³⁾ Jung et al.,⁽⁴⁾ Gungor-Winterton⁽⁵⁾ and Kandlikar-Steinke.⁽⁶⁾ A new correlation of two-phase boiling heat transfer co-

efficient in minichannel was developed based on the superposition model.

2. Experimental apparatus and methods

2.1 Experimental apparatus and method

The experimental facility is schematically shown in Fig. 1. It consisted of a condenser, a subcooler, a receiver, a pump, a mass flow meter, a preheater, and a test section. The flow rate of the refrigerant was controlled by a variable A.C output motor controller. A Coriolis-type mass flow meter was used to measure the refrigerant flow rate. To control mass quality at the test section inlet, a pre-heater was installed. For evaporation at the test section, heat fluxes were controlled using a variable A.C voltage controller. Then, vapor refrigerant from the test section was condensed in the condenser and subcooler, and then supplied to the receiver.

The test section was well insulated with rubber and foam. The outside tube wall temperatures at the top, both sides, and bottom were measured at 100 mm axial intervals from the start of the heated length with thermocouples at each measured site.

The test section was stainless steel smooth tube with the inner diameter 3.0 mm and the heated length of 2000 mm. Figure 2 shows de-

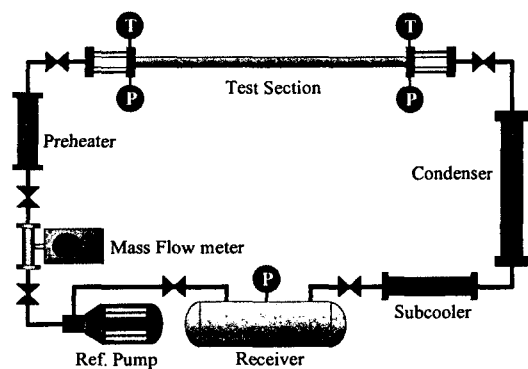


Fig. 1 The experimental test facility.

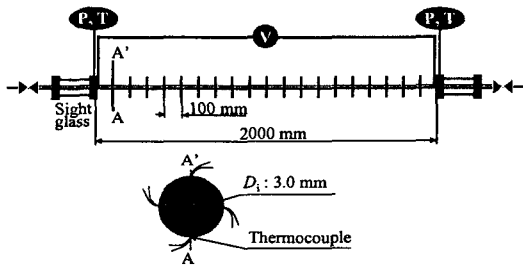


Fig. 2 The experimental test section.

tails of the experimental test section. The test section was uniformly and constantly heated by applying electric current directly to their tube wall. The input electric voltage and current were adjusted in order to control the input power. The local saturation pressure which was used to determine the saturation temperature was measured with bourdon tube type pressure gauges at the inlet and the outlet of the test section as illustrated in Figs. 1 and 2. To visualize the flow, sight glasses with the same inner diameter as the test section were installed.

The specifications of experimental test setup in this study are listed in Table 1. The physical properties of the refrigerant were obtained by referencing REFPROP 6. The temperature and flow rate data were recorded by using the Darwin DAQ32 Plus logger R9.01 software program and version 2.41 of the Micro Motion ProLink Software package, respectively.

2.2 Data Reduction

The local heat transfer coefficients at position z along the length of the test-section, were defined as

$$h = \frac{q}{T_{wi} - T_{sat}} \quad (1)$$

The inside tube wall T_{wi} was the average temperature of top, both right and left sides, and bottom wall temperatures, and determined considering radial thermal conduction through

Table 1 Experimental conditions

Refrigerants	R-134a
Test section	Horizontal stainless steel smooth tube
Inner tube diameter [mm]	3.0
Tube length [mm]	2 000
Mass flux [$\text{kg}/\text{m}^2\text{s}$]	200~600
Heat flux [kW/m^2]	10~40
Quality	0.0~1.0
Saturation temperature [$^{\circ}\text{C}$]	10

the wall,

$$T_{wi} = T_{wo} - \frac{Q}{2\pi kL} \ln \frac{D_o}{D_i} \quad (2)$$

The quality x at measurement locations z were determined based on thermodynamic properties.

$$x = \frac{i - i_f}{i_{fg}} \quad (3)$$

The refrigerant flow, at the inlet of the test section, was not completely saturated. Even though short, it was necessary to find the subcooled length for data reduction accuracy. The subcooled length was calculated with the following equation to find the initial point of saturation.

$$z_{sc} = L \frac{i_f - i_{fi}}{\Delta i} = L \frac{i_f - i_{fi}}{Q/W} \quad (4)$$

The outlet mass quality was then determined by the following equation:

$$x_0 = \frac{\Delta i + i_{fi} - i_f}{i_{fg}} \quad (5)$$

The saturation pressure at the initial point of saturation was then determined by interpolation of the measured pressure and the subcooled length.

Table 2 Summary of estimated uncertainty

Parameters	Uncertainty
T_{wi}	$\pm 0.33\%$ to $\pm 3.92\%$
P	± 2.5 kPa
G	$\pm 1.85\%$ to $\pm 3.80\%$
q	$\pm 1.79\%$ to $\pm 2.59\%$
x	$\pm 2.23\%$ to $\pm 4.19\%$
h	$\pm 2.75\%$ to $\pm 9.24\%$

Measurements were recorded with a data logger and a computer. The summary of the estimated uncertainty associated with all the parameters was tabulated in Table 2. The uncertainties changed depending on the flow conditions, from minimum to maximum.

3. Results and discussion

The experimental results were mapped on the Wojtan et al.⁽⁷⁾ and Wang et al.⁽⁸⁾ flow pattern maps. The Wojtan et al.⁽⁷⁾ flow pattern map is a modified Kattan et al.⁽⁹⁾ map, developed using R-22 and R-410A inside a 13.6 mm horizontal smooth tube. Kattan et al.⁽⁹⁾ used five refrigerants of R-134a, R-123, R-402A, R-404A, and R-502 inside 12 mm and 10.92 mm (only for R-134a) tubes, which were heated by hot water flowing counter-currently to develop their flow pattern maps on the basis of the

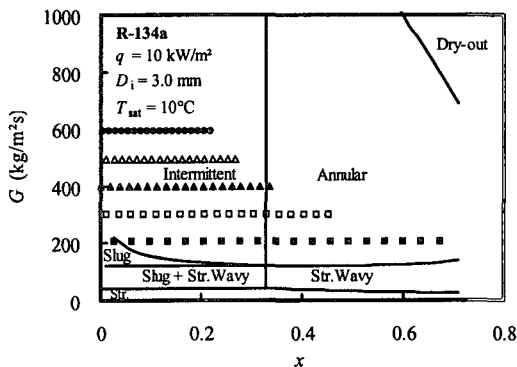


Fig. 3 The present experimental results on Wojtan et al.'s⁽⁷⁾ flow pattern map.

Steiner⁽¹⁰⁾ flow pattern map. Figure 3 depicts the present experimental results mapped on the Wojtan et al.⁽⁷⁾ flow pattern map. The experimental results mapped on the Wojtan et al.⁽⁷⁾ map are the slug, intermittent and annular flows. The flow transitions of the experimental results are shown to be delayed on the Wojtan et al.⁽⁷⁾ map.

The Wang et al.⁽⁸⁾ flow pattern map is a modified Baker map, developed using R-22, R-134a, and R-407C inside a 6.5 mm horizontal smooth tube. The Wang et al.⁽⁸⁾ map is better than the Wojtan et al.⁽⁷⁾ map to predict the flow transition of the experimental results. Figure 4 shows the present experimental results mapped on the Wang et al.⁽⁸⁾ flow pattern map. The experimental results for all the test conditions on the Wang et al.⁽⁸⁾ flow pattern map are on the intermittent, stratified wavy and annular flows. The present experimental results flow patterns with the Wang et al.⁽⁸⁾ map showed the stratified wavy flow appears at lower quality for the higher mass flux condition, and the stratified wavy regime is longer for the lower mass flux condition. The annular flow appeared earlier for higher mass flux, and the regime was longer for high mass flux condition. The results showed that mass flux had a strong effect on flow pattern but an insignificant effect of heat flux.

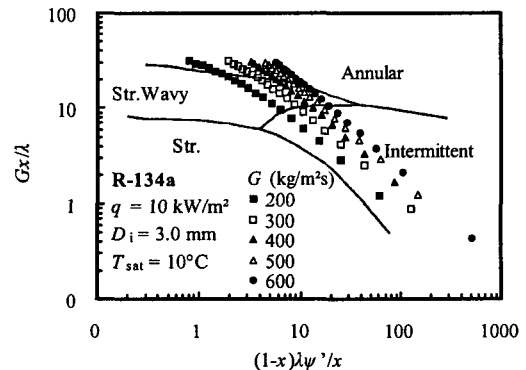


Fig. 4 The present experimental results on Wang et al.'s⁽⁸⁾ flow pattern map.

Figures 5 and 6 show that mass flux and vapor quality have no-significant effect on heat transfer coefficient at low quality; nucleate boil-

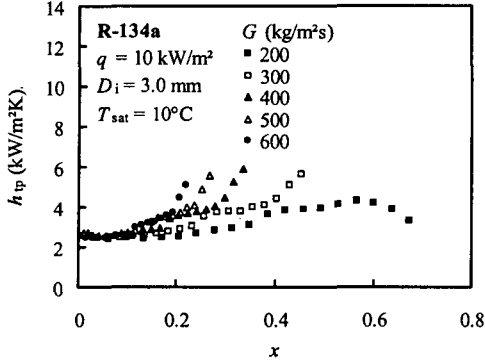


Fig. 5 The effect of mass flux on heat transfer coefficient.

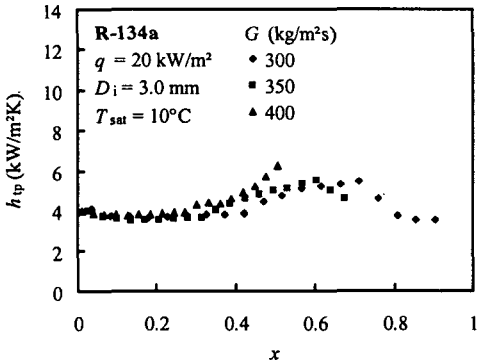


Fig. 6 The effect of mass flux on heat transfer coefficient.

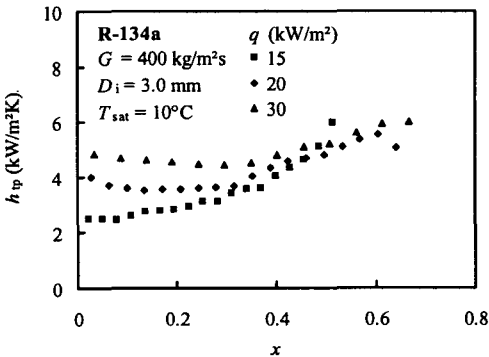


Fig. 7 The effect of heat flux on heat transfer coefficient.

ing is predominant. The significant effect of mass flux on heat transfer coefficient means a domination convective heat transfer on the total heat transfer; it is shown at higher quality. The previous studies with small tubes of Kew and Cornwell,⁽¹¹⁾ Lazarek and Black,⁽¹²⁾ Wambsgans et al.,⁽¹³⁾ Tran et al.,⁽³⁾ Bao et al.,⁽¹⁴⁾ and

Table 3 Previous correlation

Wattelet et al.⁽¹⁾

$$h_{tp} = (h_{nb}^n + h_{eb}^n)^{1/n} \quad n=2.5$$

$$h_{nb} = h_{Cooper}$$

$$h_{eb} = h_{Dittus-Boelter} \times F \times R$$

$$F = \text{fn}(X_{tt}) \quad \text{and} \quad R = \text{fn}(Fr_f)$$

Shah⁽²⁾

For horizontal tubes when $Fr_f > 0.04$

$$N = C_o = \left(\frac{1-x}{x} \right)^{0.8} \left(\frac{\rho_g}{\rho_f} \right)^{0.5}$$

$$h_{tp} = \text{MAX}(h_{nb}, h_c)$$

$$\frac{h_{nb}}{h_{fo}} = \text{fn}(N, \text{Bo}), \quad \frac{h_c}{h_{fo}} = \text{fn}(N, \text{Bo})$$

Tran et al.⁽³⁾

$$h_{tp} = 8.4 \times 10^2 (\text{Bo}^2 \text{We}_f)^{0.3} \left(\frac{\rho_f}{\rho_g} \right)^{-0.4}$$

Jung et al.⁽⁴⁾

$$h_{tp} = \frac{N}{C_{un}} h_{un} + C_{un} F_p h_{lo}$$

$$N = \text{fn}(X_{tt}, \text{Bo}), \quad \text{fn}(X, Y, p, p_{cmvc})$$

$$h_{un} = \frac{h_1 h_2}{(h_1 X_2 + h_2 X_1)}$$

$$h_1 \text{ and } h_2 \text{ are } h_{sa} = h_{\text{Stephan-Abdesalam}}$$

$$C_{me} = \text{fn}(X, Y), \quad F_p = \text{fn}(X_{tt})$$

$$h_{lo} = h_{Dittus-Boelter}$$

Gungor-Winterton⁽⁵⁾

$$h_{tp} = E \cdot h_f + S \cdot h_{pb}$$

$$E = \text{fn}(\text{Bo}, X_{tt}) \quad \text{and} \quad S = \text{fn}(\text{Bo}, X_{tt}, \text{Re}_l)$$

$$h_f = h_{Dittus-Boelter}, \quad h_{pb} = h_{Cooper}$$

Kandlikar-Steinke⁽⁶⁾

$$\frac{h_{tp}}{h_{fo}} = D_1 C_o^{D_2} (1-x)^{0.8} \text{fn}(Fr_{fo})$$

$$+ D_3 \text{Bo}_4^D (1-x)^{0.8} F_{f1}$$

$$\text{fn}(Fr_{fo})$$

Pamitran et al.⁽¹⁵⁾ showed that, in small channels, nucleate boiling was predominant; it was the opposite of the predominantly convective-dominated heat transfer of conventional channel. For the higher mass flux condition in convective boiling region, the increase of heat transfer coefficient appeared at lower quality; it can be explained that annular flow is dominant according to increase of quality. The nucleate boiling suppression appears earlier for the higher mass flux; it means that the convective heat transfer domination appears earlier for the higher mass flux condition. Heat transfer coefficients increase in annular flow region before

the initial dry-out; it can be explained that as quality increased in annular flow, the effective wall superheat decreases due to the thinner liquid film or less thermal resistance.

The dependence of heat transfer coefficients on the heat flux was high in the low quality region as illustrated in Fig.7. Nucleate boiling is known to be dominant in the initial stage of evaporation, especially for high heat flux conditions. Nucleate boiling is suppressed at high quality wherein the effect of heat flux on heat transfer coefficient becomes lower.

The heat transfer coefficients of the present study were compared against six existing two-

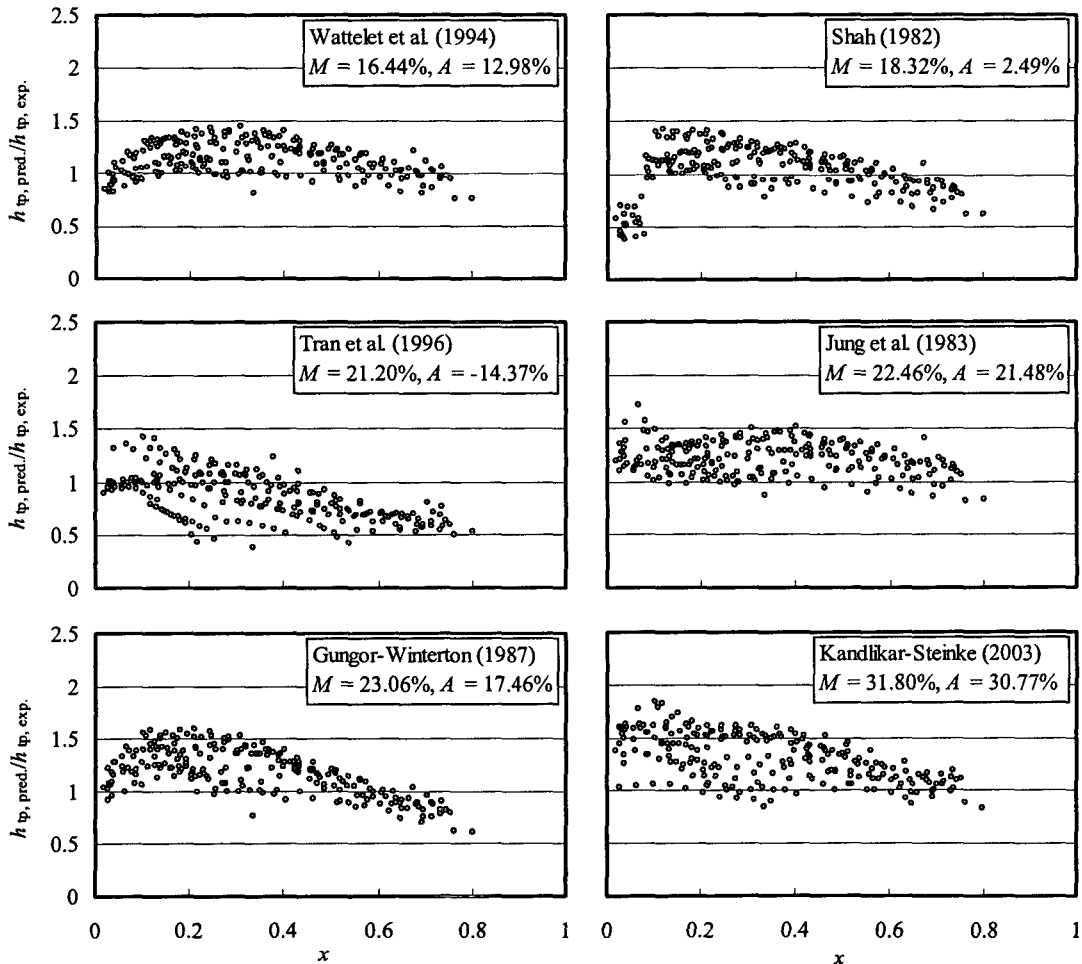


Fig. 8 The comparison of the experimental heat transfer coefficient with the existing correlations.

phase heat transfer coefficient correlations as are tabulated in Table 3. The deviation percentage of the comparison is illustrated in Fig. 8. For the overall data, the best prediction is given with the Wattelet et al.⁽¹¹⁾ method. The heat transfer deviations shown by the existing correlation is supposed due to the different size and type of experimental test section and the experimental method.

4. Development of a new correlation

4.1 Modification of factor F

As well known, the flow boiling heat transfer is governed mainly by two important mechanisms, namely: nucleate boiling and forced convective evaporation. The nucleate boiling in minichannel is higher than that in conventional channel. Therefore, the prediction of convective heat transfer contribution for refrigerant evaporation in minichannel is different from that in conventional channel. The new heat transfer coefficient correlation in this study is developed only with the experimental data prior to dry-out.

Chen⁽¹⁶⁾ introduced a multiplier factor $F = \text{fn}(X_{tt})$ to account for the increase in convective turbulence due to the presence of vapor phase. Chen⁽¹⁶⁾ correlated the factor F as a function of X_{tt} ; it should be evaluated physically again for flow boiling heat transfer in minichannel which has laminar flow condition due to the small diameter effect. By considering flow conditions (laminar or turbulent) in the Reynolds number factor F , Zhang et al.⁽¹⁷⁾ introduced a relationship between the Reynolds number factor F and the two-phase frictional multiplier based on pressure gradient for liquid alone flow ϕ_f^2 , $F = \text{fn}(\phi_f^2)$, where ϕ_f^2 is a general form for four conditions according to Chisholm,⁽¹⁸⁾

$$\phi_f^2 = 1 + \frac{C}{X} + \frac{1}{X^2} \quad (6)$$

The values of Chisholm parameter C for turbulent-turbulent (tt), laminar-turbulent (vt), turbulent-laminar (tv), and laminar-laminar (vv) are 20, 12, 10, and 5, respectively. The Martinelli parameter is defined as

$$X = \sqrt{\frac{(dp/dz)_f}{(dp/dz)_g}} = \left(\frac{f_g}{f_f}\right)^{1/2} \left(\frac{1-x}{x}\right) \left(\frac{\rho_f}{\rho_g}\right)^{1/2} \quad (7)$$

For this study, the Blasius equation of friction factor is used for the friction factors f_f and f_g , then the Martinelli parameter can be rewritten as

$$X = \left(\frac{\mu_g}{\mu_f}\right)^{1/8} \left(\frac{1-x}{x}\right)^{7/8} \left(\frac{\rho_f}{\rho_g}\right)^{1/2} \quad (8)$$

The liquid heat transfer is defined by the Dittus Boelter correlation,

$$h_{fo} = 0.023 \frac{k_f}{D} \left[\frac{G(1-x)D}{\mu_f} \right]^{0.8} \left(\frac{C_{pf} \mu_f}{k_f} \right)^{0.4} \quad (9)$$

Factor F is a convective two-phase multiplier to account for enhanced convection due to co-current flow of liquid and vapor.

A new factor F as shown in Fig. 9 is developed using the experimental data with a regression method. The new factor F can be expressed as

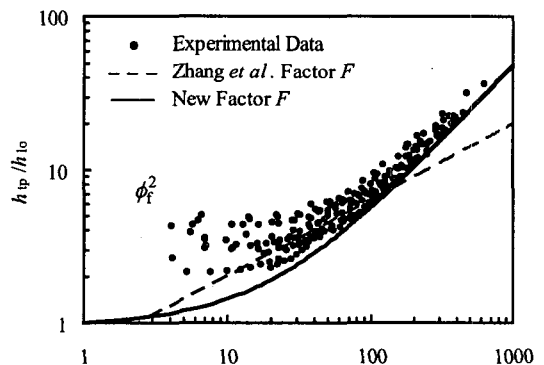


Fig. 9 Two-phase heat transfer multiplier as a function of ϕ_f^2 .

$$F = 0.048\phi_f^2 + 0.952 \quad (10)$$

where ϕ_f^2 is in Eq. (6).

4.2 Nucleate boiling contribution

Mass flux is supposed to have a high effect on the suppression of nucleate boiling. The higher mass flux is corresponding to the higher suppression of nucleate boiling. The suppression of evaporation in minichannel is lower than that in conventional channel.

The nucleate boiling heat transfer coefficient is predicted with Cooper.⁽¹⁹⁾ Cooper⁽¹⁹⁾ developed a pool boiling correlation based an extensive study. When surface roughness is set equal to $1.0\mu\text{m}$, his correlation is given as

$$h = 55P_r^{0.12}(-0.4343\ln P_r)^{-0.55} M^{-0.5} q^{0.67} \quad (11)$$

where the heat flux q is in W/m^2 and P_r is reduced pressure ($P_r = P_{sat}/P_{crit}$). The correlation covers reduced pressures from 0.001 to 0.9 and molecular weights from 2 to 200. Kew and Cornwell,⁽¹¹⁾ by using R-141b in tube with

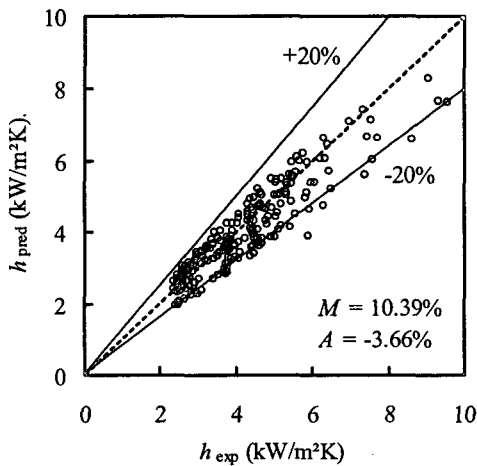


Fig. 10 Diagram of experimental heat transfer coefficient h_{exp} vs prediction heat transfer coefficient h_{pred} .

length of 500 mm and inner diameter of 1.39 to 3.69 mm, showed the Cooper⁽¹⁹⁾ pool boiling correlation best predicted their experimental data. The better prediction by using the Cooper⁽¹⁹⁾ is also shown in Jung et al.⁽²⁰⁾ study.

Chen⁽¹⁵⁾ defined the nucleate boiling suppression factor S as a ratio of the mean superheat ΔT_e to the wall superheat ΔT_{sat} . The Chen's factor S was developed with conventional channel and without using R-134a hence it needs evaluation to apply for R-134a in minichannel. Jung et al.⁽⁴⁾ proposed a convective boiling heat transfer multiplier factor N as a function of quality, heat flux, and mass flow rate (represented by employing X_{tt} and Bo) to represent the strong effect of nucleate boiling in flow boiling as it is compared to that in nucleate pool boiling, h_{nbc}/h_{pb} . To consider laminar flow in minichannels, the Martinelli parameter X_{tt} is replaced by two-phase frictional multiplier ϕ_f^2 . By using the experimental data of this study, a new nucleate boiling suppression factor, as a ratio of h_{nbc}/h_{pb} , is proposed as below:

$$S = 1.5755(\phi_f^2)^{-0.4293} \text{Bo}^{-0.0008} \quad (12)$$

4.3 Comparison of heat transfer coefficient

The new heat transfer coefficient correlation is developed by regression method with 226

Table 4 Summary of the new heat transfer coefficient correlation for R-134a

$$h_{tp} = Sh_{nbc} + Fh_{lo}$$

$$S = 1.5755(\phi_f^2)^{-0.4293} \text{Bo}^{-0.0008}$$

$$h_{nbc} = 55P_r^{0.12}(-0.4343\ln P_r)^{-0.55} M^{-0.5} q^{0.67}$$

where q is in W/m^2

$$F = 0.048\phi_f^2 + 0.952$$

$$h_{lo} = 0.023 \frac{k_f}{D} \left[\frac{G(1-x)}{\mu_f} \right]^{0.8} \left(\frac{C_{pf}\mu_f}{k_f} \right)^{0.4}$$

$$\phi_f^2 = 1 + \frac{C}{X} + \frac{1}{X^2}, \quad X = \left(\frac{\mu_f}{\mu_g} \right)^{1/8} \left(\frac{1-x}{x} \right)^{7/8} \left(\frac{\rho_g}{\rho_f} \right)^{1/2}$$

data points. The comparison of the experimental heat transfer coefficient h_{exp} and the prediction heat transfer coefficient h_{pred} is illustrated in Fig. 10. The new correlation showed a good agreement with the data with a mean deviation of 10.39% and an average deviation of -3.66%. The summary of the new correlation is shown in Table 4.

5. Concluding remarks

Convective boiling heat transfer coefficients were measured in horizontal minichannel with R-134a. Nucleate boiling heat transfer contribution was predominant at low quality region. The geometric effect of the small channel also contributes to the higher boiling nucleation. The experimental results show, at low quality region, insignificant effects of mass flux and vapor quality and a significant effect of heat flux on heat transfer coefficient. At moderate-high quality region, heat transfer coefficient for higher mass flux conditions raises and then drops at lower quality, relatively.

Because laminar flow appears on flow boiling in small channels, the modification correlation of multiplier factor on convective boiling contribution F and the nucleate boiling suppression factor S were developed in this study with laminar flow consideration. A new boiling heat transfer coefficient correlation based on the superposition model for R-134a in minichannels was presented with mean deviation of 10.39% and average deviation of -3.66%.

References

1. Wattelet, J. P., Chato, J. C., Souza, A. L. and Christoffersen, B. R., 1994, Evaporative characteristics of R-12, R-134a, and a mixture at low mass fluxes, ASHRAE Trans., 94-2-1, pp. 603-615.
2. Shah, M. M., 1982, Chart correlation for saturated boiling heat transfer: equations and further study, ASHRAE Trans., Vol. 88, pp. 185-196.
3. Tran, T. N., Wambsganss, M. W. and France, D. M., 1996, Small circular- and rectangular-channel boiling with two refrigerants, Int. J. Multiphase Flow, Vol. 22, No. 3, pp. 485-498.
4. Jung, D. S., McLinden, M., Radermacher, R. and Didion, D., 1989, A study of flow boiling heat transfer with refrigerant mixtures, Int. J. Heat Mass Transfer, Vol. 32, No. 9, pp. 1751-1764.
5. Gungor, K. E. and Winterton, H. S., 1987, Simplified general correlation for saturated flow boiling and comparisons of correlations with data, Chem. Eng. Res., Vol. 65, pp. 148-156.
6. Kandlikar, S. G. and Steinke, M. E., 2003, Predicting heat transfer during flow boiling in minichannels and microchannels, ASHRAE Trans., CH-03-13-1, pp. 667-676.
7. Wojtan, L., Ursenbacher, T. and Thome, J. R., 2005, Investigation of flow boiling in horizontal tubes: Part I-A new diabatic two-phase flow pattern map, Int. J. Heat and Mass Transfer, Vol. 48, pp. 2955-2969.
8. Wang, C. C., Chiang, C. S. and Lu, D. C., 1997, Visual observation of two-phase flow pattern of R-22, R-134a, and R-407C in a 6.5-mm smooth tube, Experimental Thermal and Fluid Science, Vol. 15, pp. 395-405.
9. Kattan, N., Thome, J. R. and Favrat, D., 1998, Flow boiling in horizontal tubes: Part 1-Development of a diabatic two-phase flow pattern map, Journal of Heat Transfer, Vol. 120, pp. 140-147.
10. Steiner, D., 1993, Heat transfer to boiling saturated liquids, VDI-Wärmeatlas (VDI Heat Atlas), Verein Deutscher Ingenieure, ed., VDI-Gesellschaft Verfahrenstechnik und Chemieingenieurwesen (GCV), Düsseldorf, Germany (J. W. Fullarton, translator).
11. Kew, P. A. and Cornwell, K., 1997, Correlations for the prediction of boiling heat transfer in small-diameter channels, Applied

- Thermal Engineering, Vol. 17(8-10), pp. 705-715.
12. Lazarek, G. M. and Black, S. H., 1982, Evaporative heat transfer, pressure drop and critical heat flux in a small diameter vertical tube with R-113, *Int. J. Heat Mass Transfer*, Vol. 25, pp. 945-960.
 13. Wambsganss, M. W., France, D. M., Jendrzeczyk, J. A. and Tran, T. N., 1993, Boiling heat transfer in a horizontal small-diameter tube, *Journal of Heat Transfer*, Vol. 115, pp. 963-975.
 14. Bao, Z. Y., Fletcher, D. F. and Haynes, B. S., 2000, Flow boiling heat transfer of freon R11 and HCFC123 in narrow passages, *Int. J. Heat and Mass Transfer*, Vol. 43, pp. 3347-3358.
 15. Pamitran, A. S., Choi, K. I., Oh, J. T. and Oh, H. K., 2006, Forced convective boiling heat transfer of R-410A in horizontal mini-channels, *Int. J. Refrigeration*, In-Press.
 16. Chen, J. C., 1966, A correlation for boiling heat transfer to saturated fluids in convective flow, *Industrial and Engineering Chemistry, Process Design and Development*, Vol. 5, pp. 322-329.
 17. Zhang, W., Hibiki, T. and Mishima, K., 2004, Correlation for flow boiling heat transfer in mini-channels, *Int. J. Heat and Mass Transfer*, Vol. 47, pp. 5749-5763.
 18. Chisholm, D., 1967, A theoretical basis for the Lockhart-Martinelli correlation for two-phase flow, *Int. J. Heat Mass Transfer*, Vol. 10, pp. 1767-1778.
 19. Cooper, M. G., 1984, Heat flow rates in saturated nucleate pool boiling—a wide-ranging examination using reduced properties, In: *Advances in Heat Transfer*, Academic Press, Vol. 16, pp. 157-239.
 20. Jung, D., Kim, Y., Ko, Y. and Song, K., 2003, Nucleate boiling heat transfer coefficients of pure halogenated refrigerants, *Int. J. Refrigeration*, Vol. 26, pp. 240-248.